Biochemistry and Biophysics Reports 12 (2017) 185–192

Contents lists available at ScienceDirect

Biochemistry and Biophysics Reports

journal homepage: www.elsevier.com/locate/bbrep

Trim33 regulates early maturation of mouse embryoid bodies in vitro

Sudha Rajderkar[1], Christopher Panaretos, Vesa Kaartinen*

Department of Biologic and Materials Sciences, University of Michigan School of Dentistry, 1011 N. University Avenue, Ann Arbor, MI 48109, USA

ARTICLE INFO

Keywords:
Tripartite motif containing 33
Apoptosis
Embryoid body maturation

ABSTRACT

Embryonic stem cells (ESCs) are an established model for investigating developmental processes, disease conditions, tissue regeneration and therapeutic targets. Previous studies have shown that tripartite motif-containing 33 protein (Trim33) functions as a chromatin reader during Nodal-induced mesoderm induction. Here we report that despite reduced proliferation, mouse ESCs deficient in *Trim33* remained pluripotent when cultured under non-differentiating conditions. However, when induced to differentiate to embryoid bodies (EBs), the mutant cultures showed increased cell shedding and apoptosis at day 3 of differentiation. *G*ene *s*et *e*nrichment *a*nalysis (GSEA) indicated that several molecular functions associated with cell survival, transcriptional/translational activity and growth factor signaling were affected already by the second day of differentiation in *Trim33*-deficient EBs. Consistent with increased apoptosis, expression of *Rac1*, a critical factor for EB cell survival, was reduced in *Trim33* mutant EBs. In addition, a set of genes involved in regulation of pluripotency was upregulated in mutant EBs. Our results suggest that Trim33 regulates early maturation of mouse embryoid bodies in vitro.

1. Introduction

Embryonic stem cells (ESCs) have been used to investigate developmental processes, disease conditions, tissue regeneration and therapeutic targets in vitro [1]. Transcriptional networks underlying ground state pluripotency have been subjects of intense studies in ESCs, and this knowledge has been effectively used for derivation of induced pluripotent cells [2–4]. During the last three decades, several key findings have contributed to the development of protocols that allow culture of non-differentiated, naïve state ESCs in vitro. Mouse ESCs are dependent on Leukemia Inhibitory Factor (LIF) and BMP signaling, while human ESCs require Fgf and Nodal/Activin signaling for successful propagation in culture in their pluripotent state [5–9]. Mouse ESCs can also be maintained in an undifferentiated state with specific small molecule inhibitors of ERK and the GSK3β kinase signaling (2i conditions) [6]. ESCs require special, defined conditions for propagation in culture in ground state pluripotency and respond to external changes by rapidly defaulting to a differentiated fate [10,11]. Here we report that in mouse ESCs, tripartite motif-containing 33 (Trim33), a tumor suppressor and transcriptional regulator, is required for early embryoid body (EB) maturation. Specifically, EBs deficient in *Trim33* showed increased apoptosis at day 3 of differentiation and already displayed notable changes in gene expression at day 2 of differentiation.

2. Materials and methods

2.1. Ethics statement

This research was conducted in strict accordance with the recommendations in the Guide for the Care and Use of Laboratory Animals of the National Institutes of Health. Experiments described are specifically approved by the University Committee on Use and Care of Animals at the University of Michigan-Ann Arbor (Protocol Number: #PRO00005004).

2.2. Establishment of embryonic stem cell lines and EB cultures

Mouse ES cells were derived from *Trim33^{FF}: UbcCre^{ERT2}* blastocysts [12] as described in [13]. ESCs were cultured on gelatin-coated culture dishes in the KSR-medium containing 15% of Knock Out Serum Replacement (Life Technologies, 10828-010), β-mercaptoethanol (1000X, Life Technologies, 21985-023), GlutaMAX-l (100X, Life Technologies, 35050-061), Penicillin/Streptomycin (Life Technologies, 15140-122) in Knockout-DMEM:Ham's F12 (1:1) in the presence of 2i + LIF (2i: PD0325901 and CHIR99021 (Stemgent) in final concentrations of 0.4 μM (or 1 μM) and 3 μM, respectively; LIF 1000 U/mL

* Corresponding author.
E-mail address: vesak@umich.edu (V. Kaartinen).
[1] Current address: MS84-171, Lawrence Berkeley National Laboratory, Berkeley, CA 94720, USA.

http://dx.doi.org/10.1016/j.bbrep.2017.10.002
Received 9 September 2016; Received in revised form 27 August 2017; Accepted 9 October 2017
Available online 18 October 2017

(Millipore, ESG 1106)). To passage the cells, the colonies were dissociated with TrypLE Express (Life Technologies, 12605-010), Trypsin was inactivated with 15% of ES-qualified FCS (Life technologies 16141-061), and cells were cultured in the KSR medium described above. Alternatively, cells were cultured in standard 2i-medium (48% NEUROBASAL (Life technologies 21103-049), 48% DMEM/F12 (Life technologies 11320-033), 0.5% N2-SUPPLEMENT (Life technologies 17502-048), 1% B27 + RA (Life technologies 17504-044), 0.65% BSA(7.5%; Life technologies 15260-037), supplemented by Penicillin/Streptomycin, GlutaMAX-l, Monothioglycerol, 1 μM PD03259010, 5 μM CHIR99021 and LIF (1000 U/mL)).

EB formation and differentiation were carried out per the ATCC protocol (http://diyhpl.us/~bryan/irc/protocol-online/protocol-cache/Embryoid_Body_Formation.pdf) in 20% serum containing medium. Both the media for non-differentiating and differentiating conditions were supplemented by GlutaMAX-l, β-mercaptoethanol and Penicillin/Streptomycin.

4-hydroxytamoxifen (4-OHT) (Sigma T176) was added at day 0 in a concentration of 1 μg/mL of medium. Some EB cultures were treated with 10 μM SB431542 (Sigma) or 20 μM Cucurbitacin I.

2.3. Western blotting

EBs were lysed in Pierce IP Lysis Buffer (ThermoScientific, Prod# 87787) supplemented with Roche proteinase inhibitor cocktail (11836153001), sodium fluoride (NaF) and sodium orthovanadate (Na_3VO_4) to a final concentration of 1 mM. Lysates were prepared per the manufacturer's instructions and used in equivalent amounts for western blotting. Antibodies used: Tfcp2l1 (R & D AF5726), Rac1 (Cytoskeleton ARCO3), Stat3 (Cell Signaling 9139) and phospho-Stat3 (Cell Signaling 9136).

2.4. Real-time PCR (qRT-PCR)

Equivalent numbers of EBs were collected in 100–200 μl of commercially available (Qiagen) RLT buffer at intended time points. RNAs were isolated using Qiagen RNeasy Mini Kit (Qiagen 74104) and cDNA was synthesized using Omniscript RT (Qiagen 205111). Taqman Assay reagents (Universal PCR 2X master mix; Applied Biosystems 4304437) were used for all targets. The reactions were quantified using Applied Biosystems ABI7300 PCR and ViiA7 detection systems and software. All Ct values were manually checked. cDNAs were diluted when necessary to avoid Cts lower than 18. Taqman Assays*: Gsc* (Mm00650681_g1)*, Nes* (Mm00450205_m1)*, Pouf51* (Mm00658129_gH)*, Mixl1 (*Mm00489085_m1), *Nanog* (Mm02019550_s1) *Trim33 (*Mm01308695_m1); all from Thermo-Fisher Scientific. *Actb:* Forward Primer (tgacaggatgcagaaggaga), Reverse Primer (cgctcaggaggagcaatg), Universal Probe #106 (Roche).

2.5. Proliferation assay

Cells plated at a density of 1×10^5 cells per cm^2 on gelatin-coated wells were fixed at 24, 48, 72 and 96-h time points with 0.5% glutaraldehyde and stained with 1% methylene blue (Sigma-Aldrich) in 0.1 M borate buffer, pH8.5 for 10 min. The stained cells were washed three times with borate buffer, color was extracted with 0.1 M HCl and absorbance was measured at 650 nm.

2.6. EB plating assay

Both control (4-OHT-) and mutant (4-OHT added at day 0) EBs were collected, washed with Ca^{2+}/Mg^{2+}-free PBS and dissociated with TrypLE at days 1 and 2 of differentiation. After cell counting, 5000, 10,000 and 20,000 cells per sample were plated on gelatin-coated 12-well plate wells as triplicates, and cultured under non-differentiation conditions in ES medium with LIF (1000 U/mL) + 2i for 2 days. Cells were fixed with 0.5% glutaraldehyde for 20 min, washed and stained with methylene blue as shown above (see Section 2.5).

2.7. RNA-Seq

Equivalent numbers of EBs were collected at day 2 and day 2.5 in triplicate mutant-control pairs in 100–200 μl commercially available (Qiagen) RLT buffer. Total RNAs were isolated using (Qiagen RNeasy Mini Kit 74104). Messenger (m)RNAs and sequencing libraries were prepared by the University of Michigan DNA Sequencing Core and reads generated on Illumina HiSeq. 2000. After quality assessment per sample, single-end, 52 base pair reads were aligned to mm9 (Mus musculus assembly July 2007) using STAR RNA Seq aligner [14]. Read counts for differential expression were obtained using the HTSeq program. Differential expression analyses were performed using the DESeq program in R Statistical Package https://bioconductor.org/packages/3.3/bioc/vignettes/DESeq/inst/doc/DESeq.pdf. HTSeq-generated read counts were separately normalized in R version 1.0.136, which uses the Trimmed Mean of M values (TMM) normalization method [15]. GEO submission GSE80166. Gene Set Enrichment Analysis (GSEA; http://www.broadinstitute.org/gsea/index.jsp) was used to identify groups of genes enriched in either control or mutant cells [16].

2.8. Immunohistochemistry

EBs were collected in sterile PBS and fixed for 15 min in freshly prepared 4% paraformaldehyde in PBS at room temperature, embedded in OCT compound and cryo-sectioned at 10 μm thickness. Primary antibodies for SSEA1 (Developmental Studies Hybridoma Bank MC480), cleaved caspase3 (Cell Signaling 9661), γH2AX (Millipore 05-636-1), Tfcp2l1 (R & D Systems AF5726), Trim33 (Sigma HPA004345), Pou5f1 (Cell signaling #2840) and laminin (Sigma L9393)) were used according to manufacturer's instructions. The specifically bound primary antibodies were detected with Alexafluor-488 or -594 secondary antibodies, and the samples were mounted in Vectashield with DAPI (Vector Labs H-1200). F-actin was stained with TRITC-Phalloidin (Sigma P1951). Fluorescent images were photographed on a Leica DMI3000B microscope with fluorescence attachments using an Olympus DP71 camera and DP controller and manager software.

2.9. Statistical analyses

For apoptosis and expression (qRT-PCR) assays, three or more samples were analyzed. Averages, standard error and probability (Student's *t*-test) were calculated and p-values of less than or equal to 0.05 were marked as significant.

3. Results and discussion

ESC lines were established from mouse embryos that were homozygous for the floxed *Trim33* allele and carried the $UbcCre^{ERT2}$ transgene ($Trim33^{FF}$:$UbcCre^{ERT2}$ ESCs). For feeder-less cultures, two separate culture conditions were tested ('KSR medium with LIF + 2i' and '2i medium with LIF + 2i'; for details see Section 2). Colony morphology, marker gene expression and growth/differentiation characteristics were comparable in both media (Supplemental Figs. 1 and 2); 'KSR medium with LIF + 2i' was used in all subsequent experiments. When $Trim33^{FF}$:$UbcCre^{ERT2}$ ESCs were exposed to 4-hydroxytamoxifen (4-OHT), sequences encoded by exons 2–4 were excised, and ESCs lacking the functional *Trim33* gene ($Trim33^{KO}$) were generated (Fig. 1A, B). $Trim33^{KO}$ ESCs were morphologically indistinguishable from control cells when cultured under non-differentiating conditions in the presence of LIF + 2i (Fig. 1 and Supplemental Fig. 1). They expressed a stem cell marker SSEA-1, the key pluripotency factor Pou5f1 (Oct4) and a naïve pluripotency marker (Tfcp2l1) [17], and showed characteristic ESC colony morphology identical to that of control mESCs (Fig. 1C-H). $Trim33^{KO}$ ESCs were propagated in culture over 20 days, corresponding to 6 passages without detectable morphological changes. However, the rate of proliferation was reduced in mutant ESCs when compared to

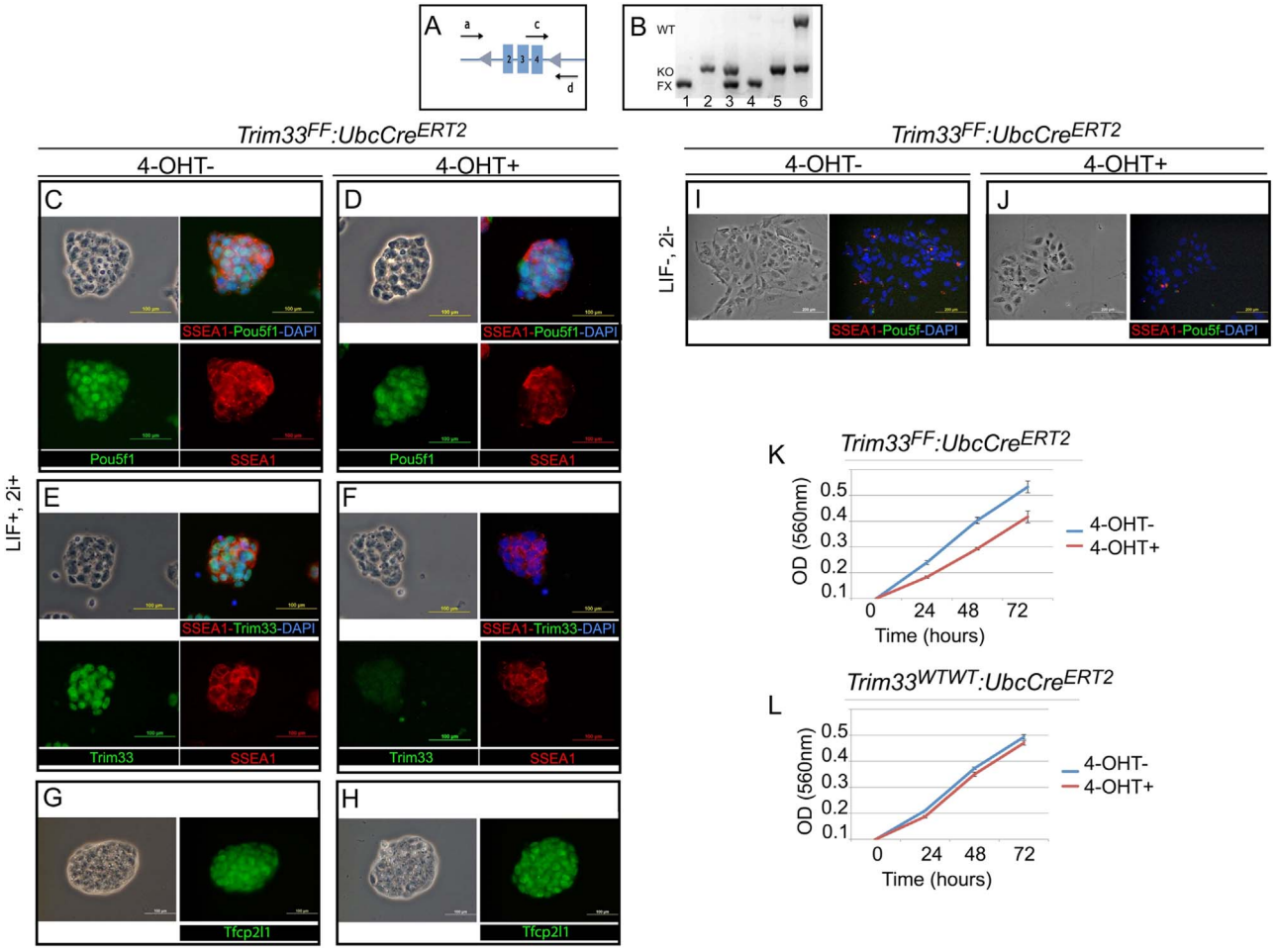

Fig. 1. Characterization of control and *Trim33*-deficient ESCs cultured under non-differentiation conditions. A, a schematic presentation of the targeted*Trim33* locus. Arrows a, c, and d depict the primers used in the genotyping assay (B). B, *Trim33^{FF}:UbcCre^{ERT2}*, 4-OHT- (1) and *Trim33^{FF}:UbcCre^{ERT2}*, 4-OHT + (2). Lanes 3–6 are known controls: #3, *Trim33^{FKO}*; #4, *Trim33^{FF}*; #5, *Trim33^{KOKO}*; #6, *Trim33^{WTKO}*. C-D, Phase contrast (top left) and immunofluorescence images for SSEA-1 (red) and Pou5f1 (green) of control (C, 4-OHT-) and *Trim33^{KO}* (D, 4-OHT +) cells showing characteristic ESC colony morphology. Cultured in the presence of LIF and 2i on gelatin-coated tissue culture dishes; top right, merge, counterstaining with DAPI (blue); bottom raw: Pou5f1 (green) and SSEA-1 (red). E-F, Phase contrast (top left) and immunofluorescence images for SSEA-1 (red) and Trim33 (green) of control (E, 4-OHT-) and *Trim33^{KO}* (F, 4-OHT +) cells showing characteristic ESC colony morphology. Cultured in the presence of LIF and 2i on gelatin-coated tissue culture dishes; top right, merge, counterstaining with DAPI (blue); bottom raw: Pou5f1 (green) and SSEA-1 (red). G-H, Phase contrast (left) and immunofluorescence images for Tfcp2l1 (right, green) of control (G, 4-OHT-) and *Trim33^{KO}* (H, 4-OHT +) cells showing characteristic ESC colony morphology. Cultured in the presence of LIF and 2i on gelatin-coated tissue culture dishes. I-J, Phase contrast and immunofluorescence images (right) for SSEA-1 (red) and Pou5f1 (green) of control (E, 4-OHT-) and *Trim33^{KO}* (F, 4-OHT +) cells cultured for 7 days without LIF and 2i on gelatin-coated tissue culture dishes. Scale bars in C-J, 100 μm. K, Proliferation curves of *Trim33^{FF}:UbcCre^{ERT2}* cells cultured in KSR with 2i + LIF for 24, 48 and 72 h; control cells (blue line), mutant cells (treated with 4-OHT for 24 h before plating (red line). L, 4-OHT-treatment of wildtype cells (*Trim33^{WTWT}:UbcCre^{ERT2}*) did not have a similar effect suggesting that reduced proliferation in *Trim33^{FF}:UbcCre^{ERT2}* cultures was not caused by 4-OHT treatment (culture conditions as in K).

controls (Fig. 1K, L). When cultured without LIF + 2i, both control and mutant cells gradually lost expression of the pluripotency markers, as expected, and showed differentiated fibroblastoid-type phenotype (Fig. 1I, J).

The critical role of TGF-β/Nodal signaling in mesendoderm induction is well-established [18]. Moreover, previous studies have shown that the function of Trim33 as a chromatin reader is required for Nodal-triggered mesendoderm induction [19]. To complement and expand these findings, we tested whether deletion of *Trim33* and inactivation of TGF-β/Nodal type I receptors (by a chemical inhibitor SB431542 [20]) would result in identical outcomes. To this end, ESCs were cultured without LIF + 2i in the presence of FCS on ultra-low attachment plates, i.e., under conditions that are permissive for ESCs to form EBs and differentiate [19]. Administration of 4-OHT at day 0 resulted in 80% reduction in Trim33 protein content at day 1, while less than 3% of Trim33 was detected at day 2 (Fig. 2A). Under these culture conditions, control ESCs (4-OHT-) formed well-defined, cystic EBs (Fig. 2B, E). In contrast, *Trim33^{FF}:UbcCre^{ERT2}* ESCs treated with 4-OHT formed EBs that showed a large number of shedding cells on the surface. These clusters gradually deteriorated and disappeared soon after the 5th day of differentiation (Fig. 2C, F). SB431542-treated cultures appeared to form differentiating EBs comparable to those in control cultures in earlier stages; however, after day 6 they lost the EB-like structure and assumed a flattened epithelium-like morphology. Clusters that survived remained attached even to low attachment dishes (Fig. 2D, G).

Since the control EBs and those cultured in the presence of 4-OHT or SB431542 appeared all morphologically different, we analyzed expression levels of well-established germ layer and pluripotency markers by using qRT-PCR. As expected, both SB431542-treated and 4-OHT-treated EBs failed to express the mesendoderm markers *Gsc* and *Mixl1*(Fig. 2H). Expression levels of pluripotency markers *Pou5f1* were markedly reduced in SB431542-treated cultures both at day 3 and day 7, when compared to control cultures while *Pou5f1* expression was sustained in 4-OHT-treated *Trim33^{KO}* cultures at identical time points (Fig. 2H). *Nanog* expression was lower both in *Trim33^{KO}* and SB431542-treated cultures (Fig. 2H).

To better understand the role of Trim33 in initial phases of EB maturation, we performed genome-wide transcriptomic analyses on

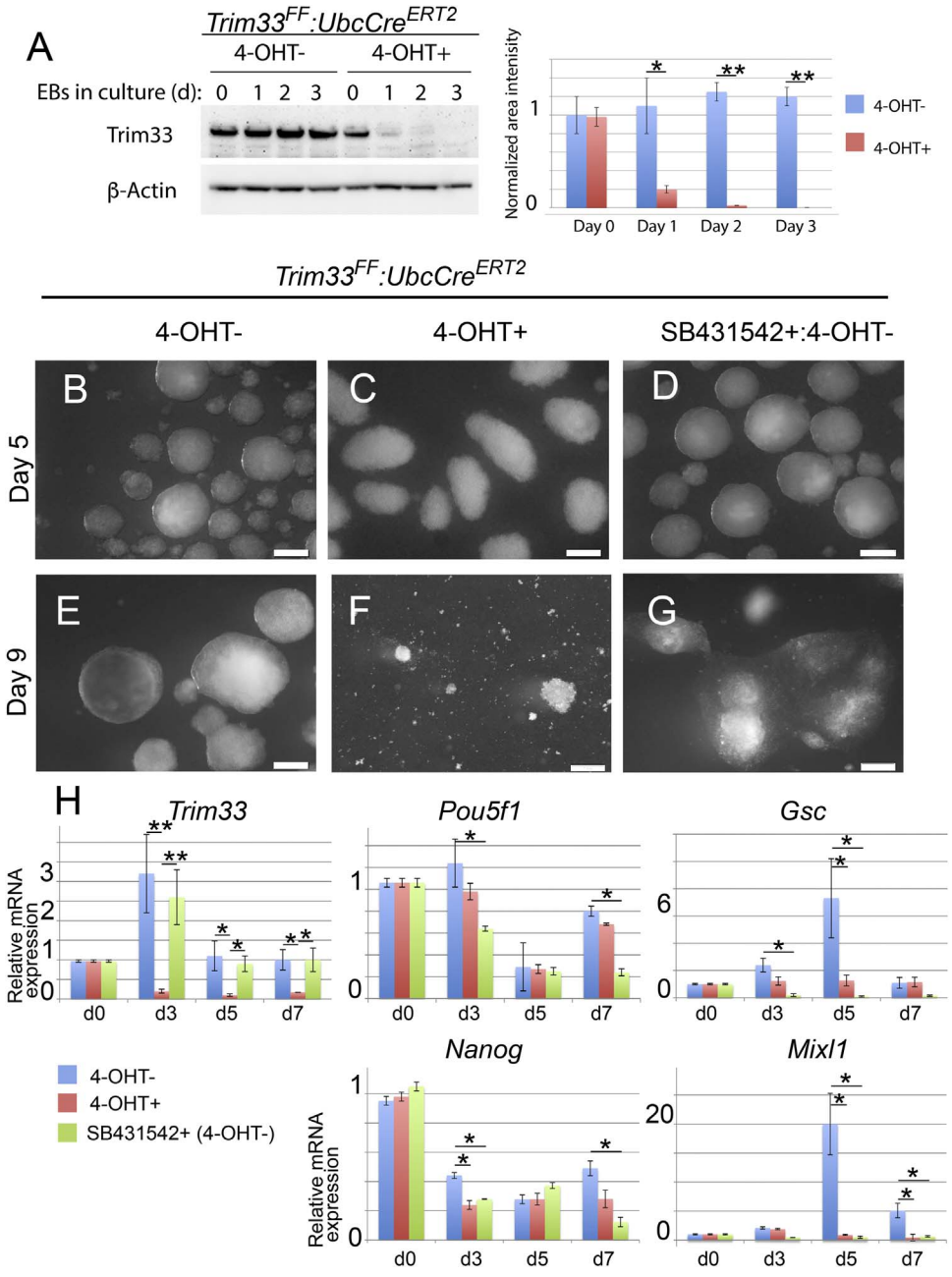

Fig. 2. *Trim33*^{KO} EBs are morphologically distinct when compared to control and SB431542-treated EBs. A, representative immuno blot (left) of control and mutant EBs during the first three days of differentiation analyzed for Trim33 (4-OHT, 1 μg/mL, was administered at day 0 of differentiation). The bar graph (right) shows relative quantification of Trim33 in control (blue bars) and mutant (red bars) (normalized to β-actin; n = 3). Error bars, S.E; * ≤ 0.05. B-G, Representative images of EBs at day 5 (B-D) and 9 (E-G) in differentiation. 4-OHT (C, F) or SB431542 (D, G) were added at the initiation of EB cultures (day 0). B, E; untreated cultures. (H) mRNA expression for *Trim33*, pluripotency markers (*Pou5f1* and *Nanog)*, mesendoderm markers (*Gsc* and *Mixl1)* in untreated EB cultures (blue bars), 4-OHT-treated EB cultures (red bars) and SB431542-treated EB cultures (green bars). Scale bars in B-D, 500 μm; E-G, 1 mm; *, p ≤ 0.05; **, p ≤ 0.01.

RNAs harvested from control and 4-OHT treated EBs (4-OHT treatment started at day 0 of differentiation). At day 2, of 56 differentially expressed genes (> 2-fold change; p ≤ 0.05, n = 3), 53 were upregulated and only three (including *Trim33)* were downregulated. Twelve hours later (day 2.5) 165 genes were downregulated and 750 genes were upregulated (Supplemental Table 1; GEO submission GSE80166). GSEA analysis revealed that gene sets associated to TAp63- and protein tyrosine phosphatase pathways, ECM-receptor interactions, apoptosis, second messenger-mediated signaling and protein kinase cascade are among the most significantly upregulated in *Trim33*^{KO} EBs at day 2 (Fig. 3A and Supplemental Table 2). In contrast, gene sets associated to mRNA splicing, RNA processing, translation factor activity, structural constituents of ribosomes, RNA Polymerase II activity and RNA processing were downregulated in mutant EBs when compared to controls (Fig. 3B). At day 2.5, gene sets associated to tissue and ectoderm development, ECM-receptor interactions, transcription factor and repressor activity and negative regulation of cell proliferation were among the most significantly enriched in mutant EBs (Fig. 3C), while gene sets associated with DNA replication, RNA splicing and processing and regulation of mitotic cell cycle were among the downregulated sets in mutants (Fig. 3D). These findings suggest that overall transcriptional and translational activities and cell survival are reduced in *Trim33*^{KO} EBs during the first three days of differentiation.

Since mutant EBs appeared non-compact and showed increased cell shedding (Fig. 2), and because GSEA assays suggested that gene sets associated with apoptosis were upregulated in *Trim33*^{KO} EBs (Fig. 3), we analyzed whether mutant EBs would show detectable differences in programmed cell death. Our assays show that even the small mutant EBs showed cleaved-caspase-3-positive apoptotic cells in the core of EBs, which normally do not show apoptosis, while the shedding cells on the surface appeared viable (Fig. 4). While the large control EBs showed some apoptotic cells in the core, as expected, the cell boundaries in control EBs appeared largely intact as shown by staining for F-actin. In contrast, massive apoptosis was associated with the loss of F-actin staining in the *Trim33* mutant EBs (Fig. 4A-D). The observed apoptosis was not caused by 4-OHT treatment or Cre-induction, since parallel

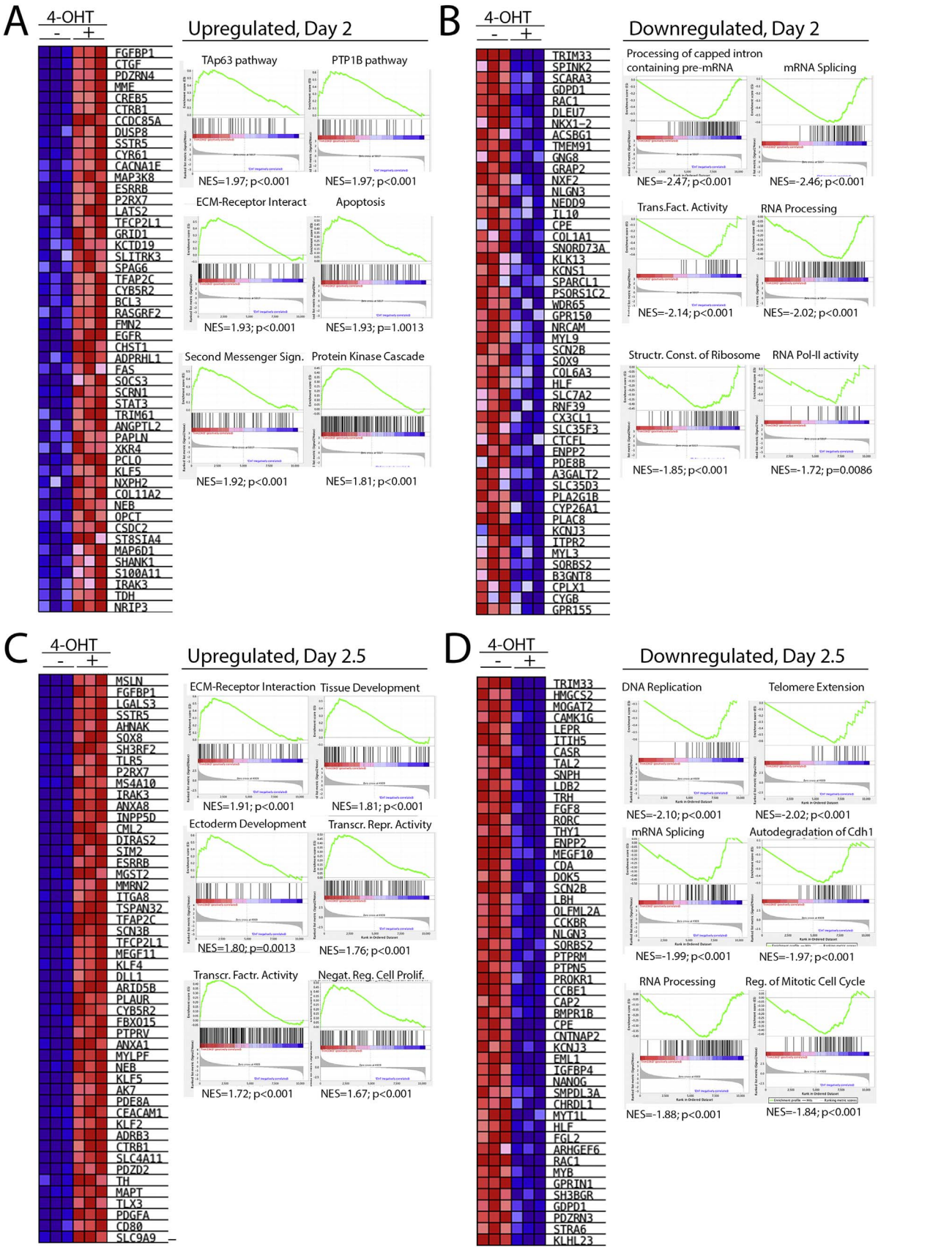

(caption on next page)

Fig. 3. Genome-wide transcriptomic analysis of control and *Trim33* mutant EBs at day 2.0 and day 2.5 of differentiation. A, GSEA-generated heat map* of top 50 genes upregulated in mutants at day 2.0 of differentiation (left). Right, examples of GSEA indicated gene sets that were upregulated in mutants at day 2.0. B, Heat map of top 50 genes downregulated in mutants at day 2.0 of differentiation (left). Right, examples of GSEA indicated gene sets that were downregulated in mutants at day 2.0. C, Heat map of top 50 genes upregulated in mutants at day 2.5 of differentiation (left). Right, examples of GSEA indicated gene sets that were upregulated in mutants at day 2.5. D, Heat map of top 50 genes downregulated in mutants at day 2.5 of differentiation (left). Right, examples of GSEA indicated gene sets that were downregulated in mutants at day 2.5. NES, normalized enrichment score. ***Please note that since GSEA considers all of the genes in an experiment, not only those above an arbitrary cutoff, the number of differentially expressed genes listed in heat maps is higher than those indicated in the main text.**

cultures, which were positive for the *UbcCre*^{ERT2} transgene and wildtype for the *Trim33* allele, were indistinguishable from the 4-OHT-negative controls (compare Fig. 4A, C and E, F). A recent study showed that *Trim33* deficiency correlates with an enhanced sensitivity to DNA damage [21]. To examine whether DNA damage would contribute to the *Trim33*^{KO} EB phenotype, we stained both control and *Trim33*^{KO} EBs for the DNA damage marker γH2AX (Fig. 4H, I). These assays revealed that there are no detectable differences in γH2AX staining between controls and *Trim33* mutants suggesting that in this context Trim33 is not involved in DNA damage response.

It was recently shown that the small Rho-related GTPase Rac1 is required for epiblast cell – basement membrane interactions in EBs and that *Rac1* deficiency results in massive apoptosis [22]. Interestingly, *Rac1* is strongly downregulated in *Trim33* mutant EBs (Figs. 3A, C and 5A, B) suggesting that reduced *Rac1* expression may contribute to the observed EB phenotype possibly by altering cell-basement membrane interactions.

As indicated above (Fig. 2), our findings are consistent with those of the previous report [19] indicating that Trim33 is required for mesoderm induction in vitro. To further explore the effect of Trim33 on expression of genes associated with mesoderm induction, we analyzed the RNA-Seq datasets for changes in established mesoderm markers. While at day 2 of differentiation, none of the mesoderm markers were differentially expressed between the controls and mutants, several of the early markers, e.g., *Brachyury* (T), *Gsc* and *Eomes* were upregulated in controls at day 2.5 of differentiation (Fig. 5). In contrast, *Brachyury* targets *Snail*-1 and *Foxa2* did not show differential expression (not shown) consistent with the fact that EBs at day 2.5 of differentiation present very early stages of mesoderm induction.

GSEA indicated several signaling pathways that were enriched in *Trim33* mutant EBs at day 2 (Table 1). In three of them, i.e., protein tyrosine phosphatase (PTP1B), protein kinase and Jak/Stat pathways, *Stat3* was upregulated. Stat3 has been shown to be a critical mediator of LIF-triggered Jak signaling, and several *Stat3* transcriptional targets have been validated as mediators of pluripotency [23–27]. Deeper examination of our RNA-Seq datasets revealed that in addition to Stat3, many of its pluripotency-associated downstream targets e.g., *Tfcp21, Klf5, Klf4, Socs3* and *Gbx2* [11,28] and other factors implicated in the regulatory network for pluripotency (*Esrrb* and *Tbx3* [11]) were upregulated in *Trim33*^{KO} EBs both at day 2 and day 2.5 of differentiation (Fig. 5).

To test whether cells of mutant EBs would be more potent in colony formation when returned to non-differentiation culture conditions, EBs were dissociated to single cells, and plated on gelatin-coated dishes in the ES culture medium supplemented with LIF and 2i (for details, see Section 2). Both control and mutant cultures established from day 1 EBs formed comparable numbers of ESC-like colonies. Consistent with the reduced proliferation rate of undifferentiated ESCs, the mutant colonies were smaller than control colonies. Both mutant and control cultures established from day 2 EBs failed to form characteristic ESC-like colonies; instead they showed attached fibroblastoid-type cells (Supplemental Fig. 3). To conclude, despite increased expression of

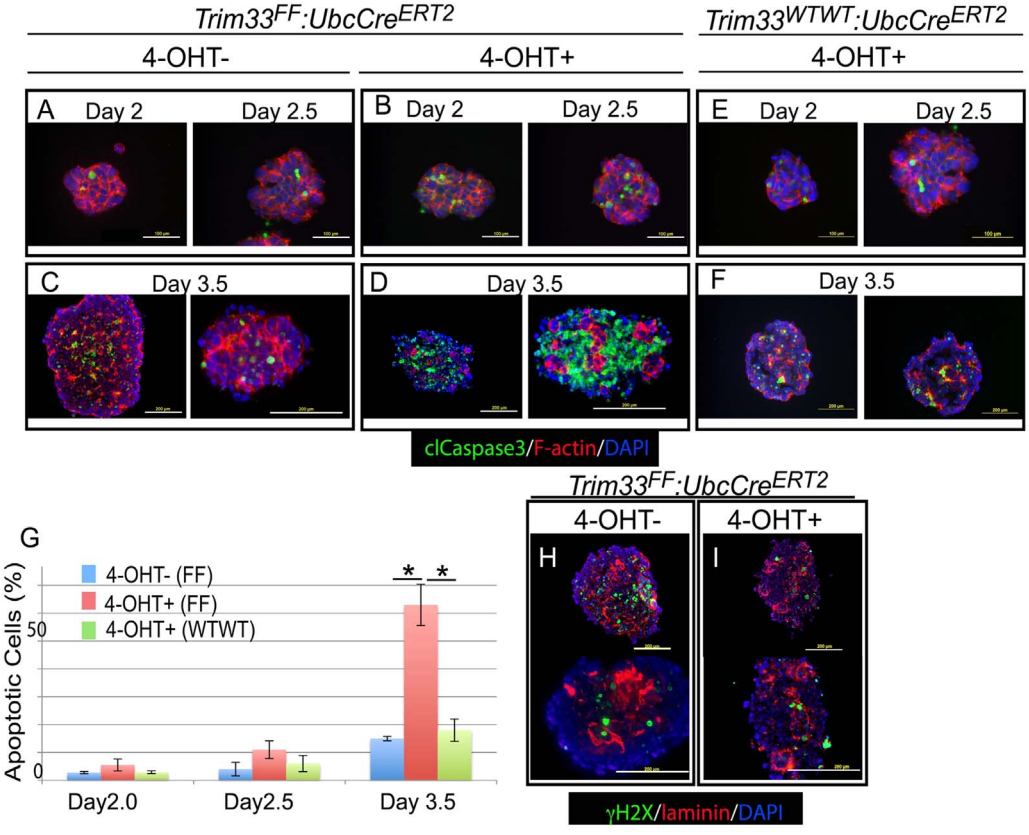

Fig. 4. *Trim33*^{KO} EBs show increased apoptosis at day 3.5 of differentiation. A-C, representative images of control (A, C) and mutant (B, D) EBs at days 2 and 2.5 of differentiation (A, B) and day 3.5 of differentiation (C and D) (4-OHT added at day 0). E, F, *Trim33*^{WTWT}*:UbcCre*^{ERT2} EBs induced with 4-OHT at day 0. Immunostaining for cleaved caspase-3 (green). To identify cell boundaries, EBs were stained for F-actin (red); nuclear counterstaining with DAPI (blue). G, Quantification of apoptotic cells; error bars, sem. H-I, representative images of control (H) and mutant (I) EBs at day 2.5 showing immunostaining for γH2AX (green); the basement membrane was stained for laminin (red); nuclear counterstaining with DAPI (blue). Scale bars, 200 μm; *, $p \leq 0.05$.

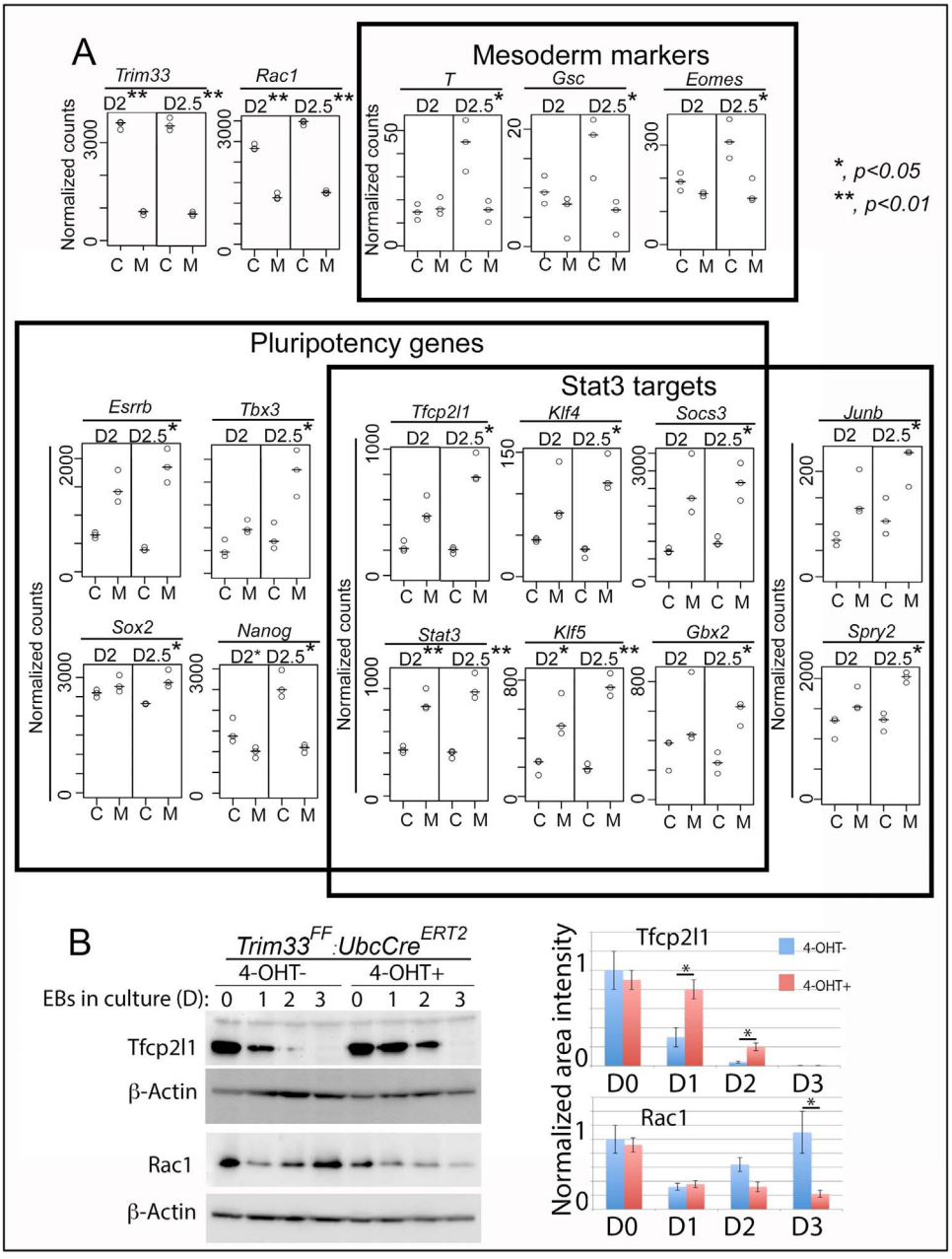

Fig. 5. Several pluripotency and Stat3 target genes are upregulated while *Rac1*, *Nanog* and mesoderm markers are downregulated in *Trim33* mutant EBs. A, Dot plots showing gene expression in normalized counts of the differentially expressed genes shown in C, control; M, mutant. Horizontal lines present the median of 3 independent findings; * ≤ 0.05; ** ≤ 0.01. B, representative immuno blot (left) of control and mutant EBs during the first three days of differentiation analyzed for the presence of Tfcp2l1 and Rac1 (4-OHT, 1 μg/mL, was administered at day 0 of differentiation). The bar graph (right) shows relative quantification of Tfcp2l1 and Rac1 in control (blue columns) and mutant (red columns) (normalized to β-actin; n = 3). Error bars, S.E; *, p ≤ 0.05; **, p ≤ 0.01.

Table 1
Top ten pathways enriched in *Trim33* mutant EBs at day 2.0 of differentiation.

Pathway	Normalized enrichment score (NES)	Nominal p-value
TAP63	1.98	P < 0.001
PTP1B*	1.97	P < 0.001
cAMP/second messenger	1.90	P < 0.001
Integrin1	1.84	P < 0.001
TNF	1.84	P = 0.0014
Protein kinase*	1.83	P = 0.0015
IL2 receptor	1.83	P < 0.001
Hedgehog	1.79	P = 0.0015
Jak/Stat*	1.66	P = 0.0097
Map kinase	1.64	P = 0.007

* *Stat3* enriched.

pluripotency associated genes in *Trim33*^{KO} EBs, their cells did not show increased or prolonged ability to form ESC-like colonies when returned to undifferentiating culture conditions suggesting that their ability of exiting the naïve state of pluripotency was not different than that of controls.

Our findings demonstrate that inducible loss of EBs deficient in *Trim33* results in increased apoptosis, the mutant EBs are morphologically distinct with notable shedding of surface cells, and display changes in gene sets associated with multiple molecular and biological processes. Since these changes have not been reported in the previous study, which used systemic *Trim33* null cells and showed that Trim33 is required for Nodal-induced mesoderm induction [19], we wondered whether the differences could be caused by different experimental strategies, i.e., systemic vs inducible gene inactivation. To this end, we induced *Trim33* deletion by 4-OHT in undifferentiated ES cells and

cultured them for 2 passages under standard ES culture conditions before starting the differentiation assay. In a parallel experiment recombination was induced at day 0 as described above. As shown in Supplemental Fig. 4, both mutant cultures showed similar phenotypes demonstrating that the observed differences between mutant and control cultures are not caused by induction of recombination simultaneously with early stages of differentiation.

Recent studies have shown that Trim33 plays a specific role in silencing transposable elements [29,30] and that at least in the mouse testis this is accomplished via specific binding to a subgroup of retrotransposons and subsequent ubiquitination and inactivation of the A-Myb transactivator [30]. Moreover, Trim33 has been shown to regulate differentiation of neural stem cells [31] and terminal differentiation of mammary epithelial cells [32]. In both contexts, Trim33 appears to control differentiation fates early on. Our present results show that Trim33 regulates early maturation events of mouse embryoid bodies. These results seem to be at odds with those of mouse embryogenesis, which showed that *Trim33* is not required for early development or mesoderm induction [33,34]. It is conceivable that experiments with ESCs in vitro remove layers of redundancy in vivo allowing discovery of novel functions for Trim33. Future studies are needed to unravel the mechanisms by which Trim33 regulates gene expression programs required for normal embryoid body maturation.

Acknowledgements

This study was supported by the NIH RO1 Grants HL074862 and DE013085 (VK). We thank Ben Ralston for technical assistance and Iros Barozzi for discussion on analyses of large datasets.

Author contributions

SR and VK designed the study, SR, CP, and VK performed the experiments, SR and VK analyzed the data and wrote the manuscript.

Appendix A. Transparency document

Transparency document associated with this article can be found in the online version at http://dx.doi.org/10.1016/j.bbrep.2017.10.002.

References

[1] M. Evans, Discovering pluripotency: 30 years of mouse embryonic stem cells, Nat. Rev. Mol. Cell Biol. 12 (2011) 680–686.
[2] D.A. Robinton, G.Q. Daley, The promise of induced pluripotent stem cells in research and therapy, Nature 481 (2012) 295–305.
[3] E. Posfai, O.H. Tam, J. Rossant, Mechanisms of pluripotency in vivo and in vitro, Curr. Top. Dev. Biol. 107 (2014) 1–37.
[4] J. Nichols, A. Smith, Naive and primed pluripotent states, Cell Stem Cell 4 (2009) 487–492.
[5] Q.L. Ying, J. Nichols, I. Chambers, A. Smith, BMP induction of Id proteins suppresses differentiation and sustains embryonic stem cell self-renewal in collaboration with STAT3, Cell 115 (2003) 281–292.
[6] Q.L. Ying, J. Wray, J. Nichols, L. Batlle-Morera, B. Doble, J. Woodgett, P. Cohen, A. Smith, The ground state of embryonic stem cell self-renewal, Nature 453 (2008) 519–523.
[7] G. Martello, A. Smith, The nature of embryonic stem cells, Annu. Rev. Cell Dev. Biol. 30 (2014) 647–675.
[8] Y. Takashima, G. Guo, R. Loos, J. Nichols, G. Ficz, F. Krueger, D. Oxley, F. Santos, J. Clarke, W. Mansfield, W. Reik, P. Bertone, A. Smith, Resetting transcription factor control circuitry toward ground-state pluripotency in human, Cell 158 (2014) 1254–1269.
[9] T.W. Theunissen, M. Friedli, Y. He, E. Planet, R.C. O'Neil, S. Markoulaki, J. Pontis, H. Wang, A. Iouranova, M. Imbeault, J. Duc, M.A. Cohen, K.J. Wert, R. Castanon, Z. Zhang, Y. Huang, J.R. Nery, J. Drotar, T. Lungjangwa, D. Trono, J.R. Ecker, R. Jaenisch, Molecular criteria for defining the naive human pluripotent state, Cell Stem Cell 19 (2016) 502–515.
[10] C. Mulas, T. Kalkan, A. Smith, NODAL secures pluripotency upon embryonic stem cell progression from the ground state, Stem Cell Rep. 9 (2017) 77–91.
[11] T. Kalkan, N. Olova, M. Roode, C. Mulas, H.J. Lee, I. Nett, H. Marks, R. Walker, H.G. Stunnenberg, K.S. Lilley, J. Nichols, W. Reik, P. Bertone, A. Smith, Tracking the embryonic stem cell transition from ground state pluripotency, Development 144 (2017) 1221–1234.
[12] Y. Ruzankina, C. Pinzon-Guzman, A. Asare, T. Ong, L. Pontano, G. Cotsarelis, V.P. Zediak, M. Velez, A. Bhandoola, E.J. Brown, Deletion of the developmentally essential gene ATR in adult mice leads to age-related phenotypes and stem cell loss, Cell Stem Cell 1 (2007) 113–126.
[13] T. Pieters, L. Haenebalcke, T. Hochepied, J. D'Hont, J.J. Haigh, F. van Roy, J. van Hengel, Efficient and user-friendly pluripotin-based derivation of mouse embryonic stem cells, Stem Cell Rev. 8 (2012) 768–778.
[14] A. Dobin, C.A. Davis, F. Schlesinger, J. Drenkow, C. Zaleski, S. Jha, P. Batut, M. Chaisson, T.R. Gingeras, STAR: ultrafast universal RNA-seq aligner, Bioinformatics 29 (2013) 15–21.
[15] M.D. Robinson, A. Oshlack, A scaling normalization method for differential expression analysis of RNA-seq data, Genome Biol. 11 (2010) R25.
[16] A. Subramanian, P. Tamayo, V.K. Mootha, S. Mukherjee, B.L. Ebert, M.A. Gillette, A. Paulovich, S.L. Pomeroy, T.R. Golub, E.S. Lander, J.P. Mesirov, Gene set enrichment analysis: a knowledge-based approach for interpreting genome-wide expression profiles, Proc. Natl. Acad. Sci. USA 102 (2005) 15545–15550.
[17] L. Weinberger, M. Ayyash, N. Novershtern, J.H. Hanna, Dynamic stem cell states: naive to primed pluripotency in rodents and humans, Nat. Rev. Mol. Cell Biol. 17 (2016) 155–169.
[18] F.L. Conlon, K.M. Lyons, N. Takaesu, K.S. Barth, A. Kispert, B. Herrmann, E.J. Robertson, A primary requirement for nodal in the formation and maintenance of the primitive streak in the mouse, Development 120 (1994) 1919–1928.
[19] Q. Xi, Z. Wang, A.I. Zaromytidou, X.H. Zhang, L.F. Chow-Tsang, J.X. Liu, H. Kim, A. Barlas, K. Manova-Todorova, V. Kaartinen, L. Studer, W. Mark, D.J. Patel, J. Massague, A poised chromatin platform for TGF-beta access to master regulators, Cell 147 (2011) 1511–1524.
[20] G.J. Inman, F.J. Nicolas, J.F. Callahan, J.D. Harling, L.M. Gaster, A.D. Reith, N.J. Laping, C.S. Hill, SB-431542 is a potent and specific inhibitor of transforming growth factor-beta superfamily type I activin receptor-like kinase (ALK) receptors ALK4, ALK5, and ALK7, Mol. Pharmacol. 62 (2002) 65–74.
[21] A. Kulkarni, J. Oza, M. Yao, H. Sohail, V. Ginjala, A. Tomas-Loba, Z. Horejsi, A.R. Tan, S.J. Boulton, S. Ganesan, Tripartite Motif-containing 33 (TRIM33) protein functions in the poly(ADP-ribose) polymerase (PARP)-dependent DNA damage response through interaction with Amplified in Liver Cancer 1 (ALC1) protein, J. Biol. Chem. 288 (2013) 32357–32369.
[22] X. He, J. Liu, Y. Qi, C. Brakebusch, A. Chrostek-Grashoff, D. Edgar, P.D. Yurchenco, S.A. Corbett, S.F. Lowry, A.M. Graham, Y. Han, S. Li, Rac1 is essential for basement membrane-dependent epiblast survival, Mol. Cell Biol. 30 (2010) 3569–3581.
[23] O. Gafni, L. Weinberger, A.A. Mansour, Y.S. Manor, E. Chomsky, D. Ben-Yosef, Y. Kalma, S. Viukov, I. Maza, A. Zviran, Y. Rais, Z. Shipony, Z. Mukamel, V. Krupalnik, M. Zerbib, S. Geula, I. Caspi, D. Schneir, T. Shwartz, S. Gilad, D. Amann-Zalcenstein, S. Benjamin, I. Amit, A. Tanay, R. Massarwa, N. Novershtern, J.H. Hanna, Derivation of novel human ground state naive pluripotent stem cells, Nature 504 (2013) 282–286.
[24] H. Niwa, T. Burdon, I. Chambers, A. Smith, Self-renewal of pluripotent embryonic stem cells is mediated via activation of STAT3, Genes Dev. 12 (1998) 2048–2060.
[25] T. Matsuda, T. Nakamura, K. Nakao, T. Arai, M. Katsuki, T. Heike, T. Yokota, STAT3 activation is sufficient to maintain an undifferentiated state of mouse embryonic stem cells, EMBO J. 18 (1999) 4261–4269.
[26] C.B. Ware, A.M. Nelson, B. Mecham, J. Hesson, W. Zhou, E.C. Jonlin, A.J. Jimenez-Caliani, X. Deng, C. Cavanaugh, S. Cook, P.J. Tesar, J. Okada, L. Margaretha, H. Sperber, M. Choi, C.A. Blau, P.M. Treuting, R.D. Hawkins, V. Cirulli, H. Ruohola-Baker, Derivation of naive human embryonic stem cells, Proc. Natl. Acad. Sci. USA 111 (2014) 4484–4489.
[27] D. Qiu, S. Ye, B. Ruiz, X. Zhou, D. Liu, Q. Zhang, Q.L. Ying, Klf2 and Tfcp2l1, two wnt/beta-catenin targets, act synergistically to induce and maintain naive pluripotency, Stem Cell Rep. 5 (2015) 314–322.
[28] P.Y. Bourillot, I. Aksoy, V. Schreiber, F. Wianny, H. Schulz, O. Hummel, N. Hubner, P. Savatier, Novel STAT3 target genes exert distinct roles in the inhibition of mesoderm and endoderm differentiation in cooperation with Nanog, Stem Cells 27 (2009) 1760–1771.
[29] B. Herquel, K. Ouararhni, I. Martianov, S. Le Gras, T. Ye, C. Keime, T. Lerouge, B. Jost, F. Cammas, R. Losson, I. Davidson, Trim24-repressed VL30 retrotransposons regulate gene expression by producing noncoding RNA, Nat. Struct. Mol. Biol. 20 (2013) 339–346.
[30] L. Isbel, R. Srivastava, H. Oey, A. Spurling, L. Daxinger, H. Puthalakath, E. Whitelaw, Trim33 binds and silences a class of young endogenous retroviruses in the mouse testis; a novel component of the arms race between retrotransposons and the host genome, PLoS Genet. 11 (2015) e1005693.
[31] S. Falk, E. Joosten, V. Kaartinen, L. Sommer, Smad4 and trim33/tif1gamma redundantly regulate neural stem cells in the developing cortex, Cereb. Cortex 24 (2014) 2951–2963.
[32] C. Hesling, J. Lopez, L. Fattet, P. Gonzalo, I. Treilleux, D. Blanchard, R. Losson, V. Goffin, N. Pigat, A. Puisieux, I. Mikaelian, G. Gillet, R. Rimokh, Tif1gamma is essential for the terminal differentiation of mammary alveolar epithelial cells and for lactation through SMAD4 inhibition, Development 140 (2013) 167–175.
[33] L. Morsut, K.P. Yan, E. Enzo, M. Aragona, S.M. Soligo, O. Wendling, M. Mark, K. Khetchoumian, G. Bressan, P. Chambon, S. Dupont, R. Losson, S. Piccolo, Negative control of Smad activity by ectodermin/Tif1gamma patterns the mammalian embryo, Development 137 (2010) 2571–2578.
[34] J. Kim, V. Kaartinen, Generation of mice with a conditional allele for Trim33, Genesis 46 (2008) 329–333.